



# Strike-slip faulting in extending upper plates: insight from the Aegean

Agathe Faucher<sup>1</sup>, Frédéric Gueydan<sup>1</sup>, Jeroen Van Hunen<sup>2</sup>

<sup>1</sup>Géosciences Montpellier, Université de Montpellier, CNRS, Rue Eugène Bataillon, 34095 Montpellier, France

<sup>2</sup>Department of Earth Sciences, University of Durham, Durham DH1 3LE, United Kingdom

5 *Correspondence to:* Frédéric Gueydan (frederic.gueydan@umontpellier.fr)

**Abstract.** During gravitational collapse of orogenic systems or in hot extending back-arc systems, normal faulting is often associated with strike slip faulting whose origin remains enigmatic. The formation of major strike slip fault zones during subduction upper plate extension driven by slab-roll back can be related to slab tearing at depth. In the Aegean, where back-arc extension driven by southwest-ward migration of the Hellenic trench (slab rollback) has occurred since at least 30 Ma, the co-existence of normal faulting and a multiple strike-slip fault zones is observed since the onset of the westward extrusion of Anatolia, but before the onset of slab tearing that occurs in the Pliocene. Here we show how strike slip faults and normal faults can coexist in a hot deforming continental lithosphere. Our 3D numerical models with two deformation stages (initial pure extension followed by combined shortening and extension) can explain the Aegean tectonics. Several rifts form during the purely extensional stage that, during the second deformation stage, are either fully reactivated as strike-slip faults, or remain active but rimmed by dextral and sinistral strike-slip faults. This suggests that the extension driven by slab rollback and shortening driven by westward extrusion of Anatolia interact in space and time in the Aegean domain to create a complex tectonic pattern with coeval active normal faulting (e.g. Corinth and Evvia rifts) and dextral strike-slip faulting (e.g. the North Anatolian and Myrthes-Ikaria faults). These results show that strike slip faults in extending domain can be a sign of shortening at high angle to the extension direction.

## 20 1 Aegean tectonics

Upper plate extension driven by slab rollback is a typical feature of subduction systems. The Mediterranean shows that such extension in the continental upper plate leads to normal faulting, crustal thinning (Alboran, Aegean) and back-arc basins (Liguro-Provençal, Tyrrhenian; see Royden and Faccenna, 2018). In these extended back-arc domains, strike-slip faults are observed (e.g. the Carbonera fault in the Alboran, Rutter et al., 2012; or the Alfeo fault systems in the Ionian sea, Gutscher et al., 2016). The Eastern-Mediterranean system is marked by a large strike-slip fault system (Fig. 1C, Sakellariou and Tsampouraki-Kraounaki, 2018). Some of these faults have obvious origins. The Kefalonia fault is associated with STEP faulting (Govers and Wortel, 2005) above a slab tear (Royden and Papanikolaou, 2011). The North Anatolian fault (NAF) is

commonly assumed to have propagated westward during the Plio-Quaternary and to fully accommodate the extrusion of Anatolia (Armijo et al., 1999). The Aegean domain shows, however, a large number of other strike slip faults (Pelagonian, Myrthes-Ikaria, Amorgos , Fig. 1C) that requires a different explanation.

30 Myrthes-Ikaria, Amorgos , Fig. 1C) that requires a different explanation.

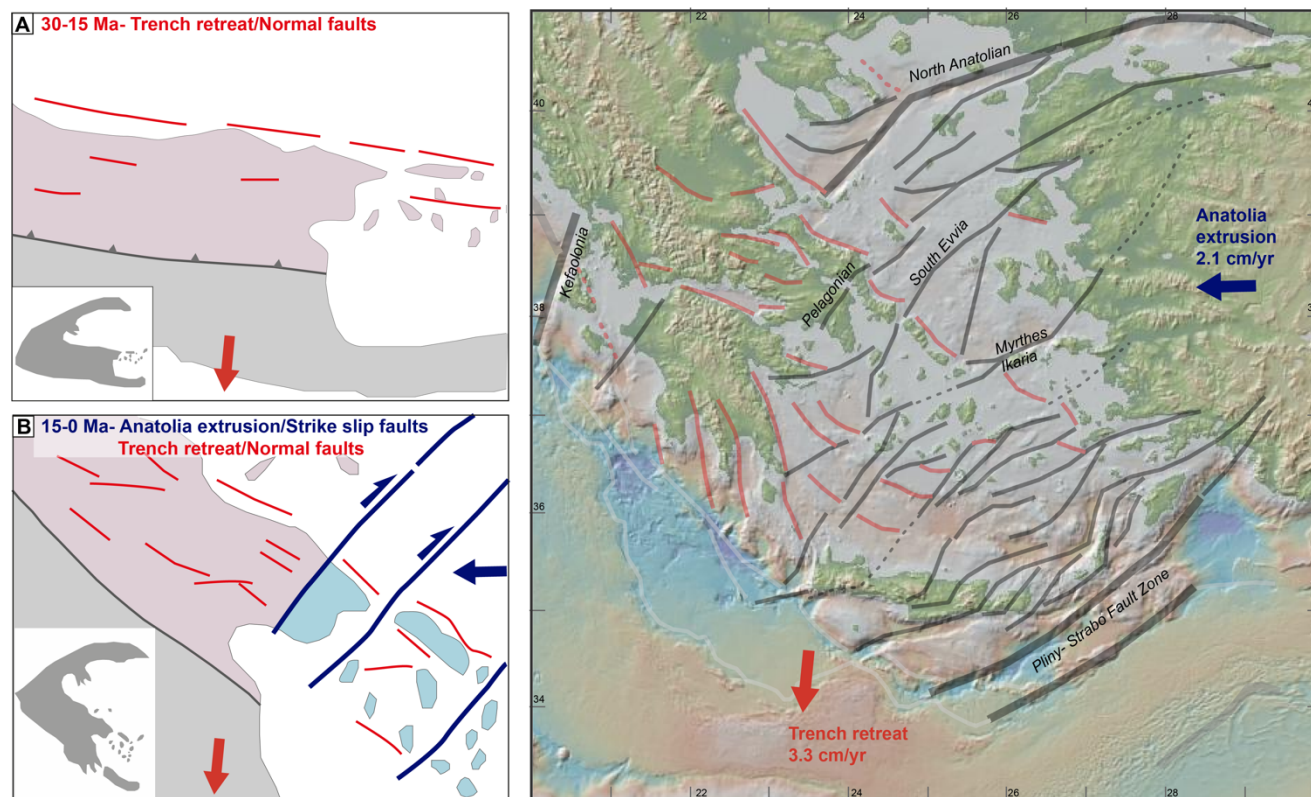


**Figure 1: Neogene Aegean tectonics with the interaction between southwestward Hellenic trench retreat and westward Anatolia extrusion. A/ 30-15 Ma stage of deformation: only normal faulting driven by trench retreat. B/ 15-5 Ma stage of deformation: coeval N-S extension (trench retreat) and E-W shortening (Anatolia extrusion) with coexistence of normal faults and dextral strike-slip faults. C/ Present day configuration with key faults (dextral strike-slips in black and normal faults in red).**

35

The present-day tectonics of the Aegean micro-plate is controlled by southwestward Hellenic trench retreat at 3.2 cm/yr and westward Anatolia escape at 2.1 cm/yr (with respect to stable Eurasia, Fig. 1C, Reilinger et al., 2006). The Hellenic subduction has been active since Jurassic times, and southward slab rollback initiated in the Oligocene/Eocene and is  
40 accommodated by Aegean upper plate extension (Fig. 1A, 30-15 Ma, see Brun et al., 2016 for a review). The formation of

metamorphic core complexes (Rhodopes in Oligocene and Cyclades in Miocene) highlights the high geothermal gradient in the Aegean domain during extension.

In the Mid-Miocene, collision between Arabia and Eurasia triggered the onset of westward motion of Anatolia (Şengör et al., 2005) that interacted with back-arc extension in the Aegean domain (Fig. 1B). Recent ages on calcite precipitation in the eastern portion of the North Anatolian Fault suggest its Mid-Miocene activity (Nuriel et al., 2019). Moreover, Mid-Miocene plutons in the Cyclades show syn-kinematics deformation, suggesting a dextral strike-slip deformation during their emplacement along the Myrthes-Ikaria strike-slip fault system (Fig. 1C, Kokkalas and Aydin, 2013). Furthermore, low temperature ages coupled with tectonic observations support a mid-Miocene strike slip activity of the Pelagonian fault in Evvia and Attica (Fig. 1C, Faucher et al., 2020). Strike-slip faulting was therefore active coevally with normal faulting in Miocene times, when both N-S extension and E-W shortening occurred (Fig. 1B). In the Plio-Quaternary, a plate re-organization occurred, with the formation of the Corinth and Evvia rifts, the Kefhalonia fault zones and the localization of deformation in the Aegean domain towards the North Anatolian fault, forming the Aegean/Anatolia microplate (Fig. 1C, Pérouse et al., 2015). This kinematic reorganization may have been triggered by slab tearing beneath Kefhalonia (Bocchini et al., 2018), which may provide a possible explanation for the origin of strain localization towards the NAF (Sternai et al., 2014). However, the Miocene activity of the NAF and the existence of numerous active dextral strike-slip faults (Fig. 1C) during the Miocene (e.g. before slab tearing) question the origin of strike-slip faulting in the Aegean domain.

Our objective is therefore to quantify the mechanical and kinematical conditions for the coexistence of strike slip and normal faults in a deforming continental lithosphere. We wish to test if the combination of extension and compression intrinsically leads to the development of both normal faults and strike-slip faults, as suggested by the Miocene deformation stage in the Aegean domain (Fig. 1B). Extension rates at that time were lower than the present-day rate and most probably close to the extrusion rate (Brun et al., 2016). Analogue models have suggested a possible nucleation of strike-slip faults in such settings (Philippon et al, 2014), but with inherited structures. Here we aim to explore, using simple 3D lithosphere-scale numerical models, the self-consistent triggering of strike-slip faulting purely by the coeval activity of extension and shortening.

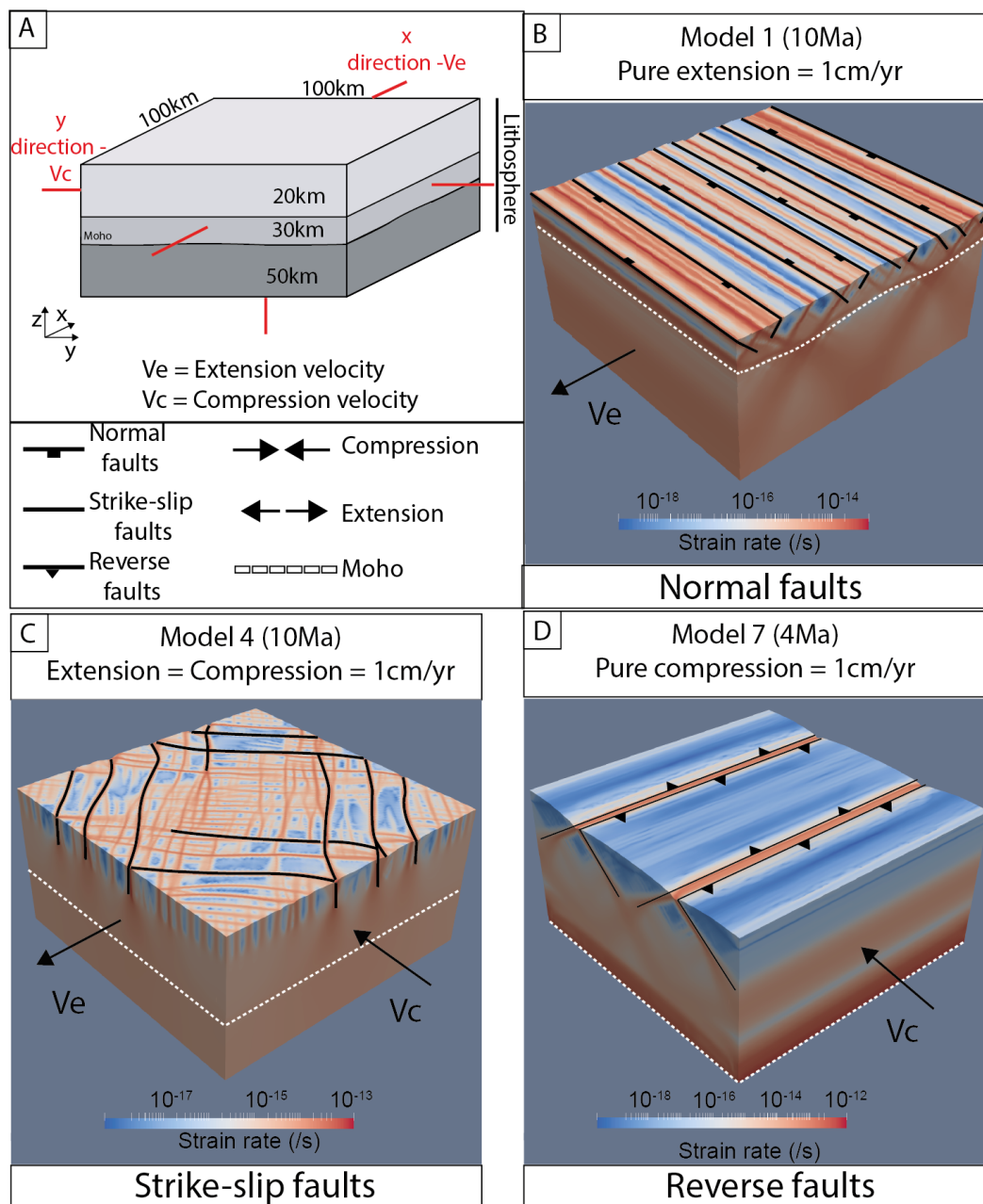


## 65 2. Model set-up and 3D end-members models.

We select a hot initial geotherm with a Moho temperature at 920°C, yielding a lithosphere thickness of 50 km. Despite the large amount of extension since 30 Ma, the Moho is almost flat in a large part of the Aegean domain (Tirel et al., 2004), suggesting wide rifting/metamorphic core complex mode of extension, typical of hot lithosphere (Buck, 1991). The large  
70 present-day surface heat flow (Cloetingh et al., 2010) furthermore suggests a Moho temperature around 850-950°C, consistent with crustal anatexis and magmatism (Menant et al., 2016).

The modelled box size is therefore 50 km thick, and 100 km wide in x- and y-direction (Fig. 2A). Extension velocity  $V_e$  is applied in the x-direction (i.e. at the two vertical boundaries orthogonal to x), and compression velocity  $V_c$  in y-direction (i.e. at the two vertical boundaries orthogonal to y). Material can freely exit or enter from the bottom or the vertical sides, to  
75 allow thickening or thinning. The crust and mantle materials are composed of quartz and olivine, respectively, with different rheological parameters, density and thermal conductivity (Tab. S1). The mesh is refined at the level of the crust (2 km x 2 km) compared to the mesh of the mantle (4 km x 4 km), for high-resolution of the faults. Crustal anatexis, which should occur at such high geotherm, is not included for the sake of simplicity.

The hot geotherm results in a rheological layering that is typical for such lithosphere: a thin brittle crust (7 km), and a viscous  
80 mantle underneath (Fig. S2). A distinction between the upper (20 km) and lower (10 km) crust is made based on the difference in the rate of radiogenic elements (Fig. 2A and Tab. S1). Computations were done using the geodynamical finite-element ASPECT code version 2.5.0, see Kronbichler et al., 2012; Heister et al., 2017; Bangerth et al., 2022, 2023) to solve the system of equations for highly viscous fluid motion. The rheological model combines dislocation creep with Drucker-Prager plasticity.



85

90

**Figure 2:** 3D model of hot lithosphere deformation under pure extension, pure shortening and shortening+extension. **A/** Model setup with material layering and boundary conditions, with extension at  $V_e$  in the x-direction and compression at  $V_c$  in the y-direction. At the bottom, an inflow velocity is imposed to ensure constant volume during deformation. **B/** Strain rate after 10 Myr for Model  $M_e$  with only extension ( $V_e=1$  cm/yr,  $V_c=0$ ). Main normal faults drawn in black. **C/** Strain rate after 10 Myr for Model  $M_{ec}$  with both extension and compression ( $V_e=1$  cm/yr,  $V_c=1$  cm/yr). Main strike-slip faults drawn in black. **D/** Strain rate after 4 Ma for Model  $M_c$  with only compression ( $V_e=0$ ,  $V_c=1$ cm/yr). Main thrusts in black. The Moho is drawn as a white, dashed line. Input files for the three models can be found in Faucher et al. (2024).



95 Figure 2 presents three end-member solutions: pure extension (model  $M_e$ ,  $V_e=1\text{cm/yr}$ ,  $V_c=0$ ), pure shortening (model  $M_c$ ,  $V_c=1\text{ cm/yr}$ ) and equal extension/shortening (model  $M_{ec}$ ,  $V_e=V_c=1\text{cm/yr}$ ).

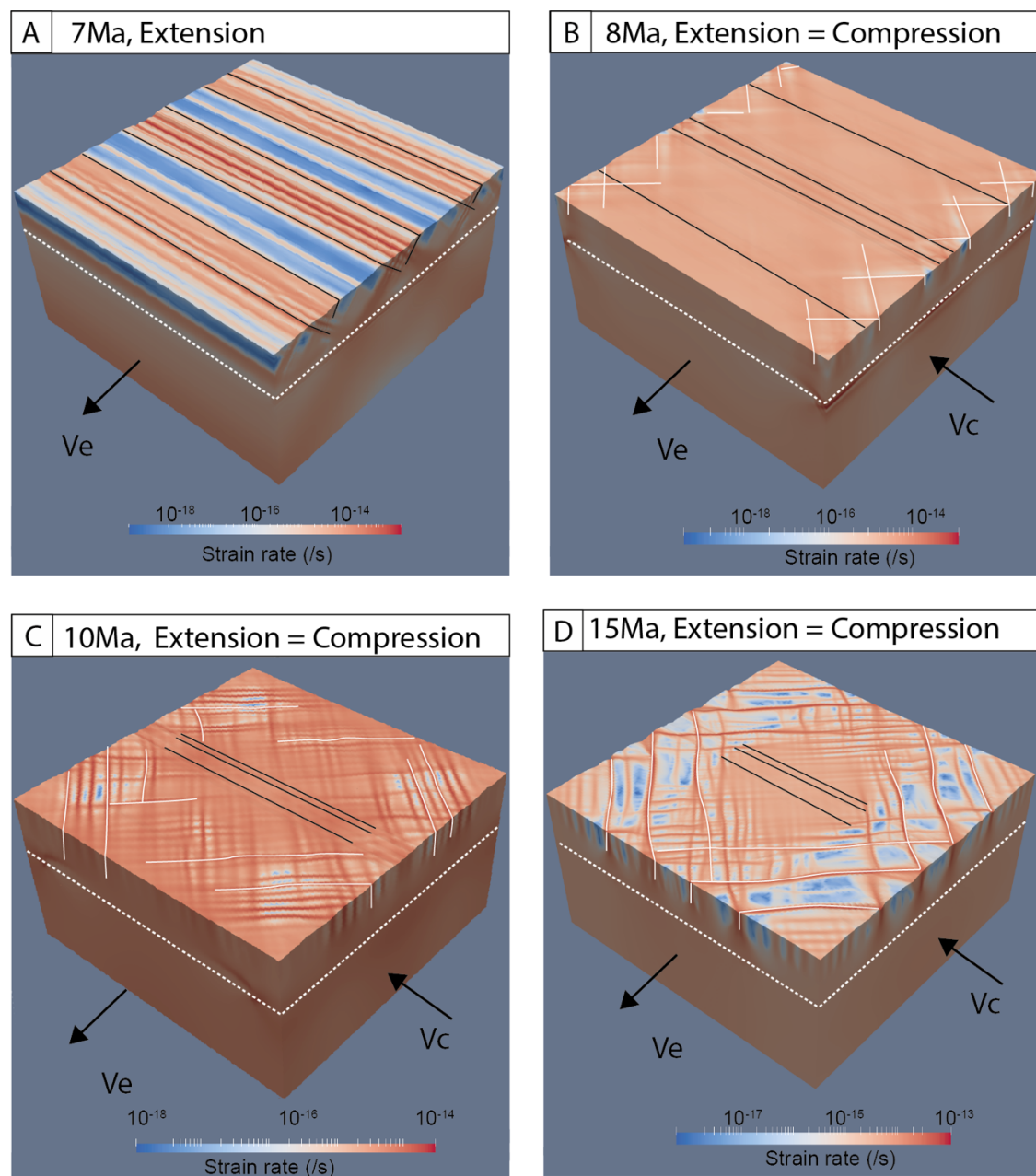
Model  $M_e$  (after 10 Myr of extension, i.e. 100 km of purely extensional displacement, Fig. 2B) shows numerous normal faults perpendicular to the stretching direction in a distributed way inside the model. This reflects the wide rifting mode of deformation due to the high Moho temperature and hence the absence of brittle mantle lithosphere (Buck, 1991; Gueydan et al., 2008). The homogeneous ductile deformation of the subcontinental mantle implies homogeneous deformation of the crust and hence formation of numerous faults in the upper crust..

Model  $M_c$  (after 4 Myr, e.g. 40 km of purely compressional displacement, Fig. 2D) shows two deformation zones, defined by two conjugate thrusts, developing orthogonal to the direction of compression. The hanging walls of these faults have a high topography. The footwalls of the two conjugate thrusts experience a downward vertical motion of a triangular shaped portion of the crust. This pop-down like structure leads to homogeneous thickening of the crust, typical of hot lithosphere compression (Cagnard et al., 2006).

Model  $M_{ec}$  ( $V_c=V_e=1\text{ cm/yr}$ ) implies no net inflow or outflow of material from the bottom of the model and develops a constant crustal thickness in time. After 10 Myr, the upper crust is marked by numerous vertical faults, at  $35^\circ$  to  $45^\circ$  to the shortening and extension directions (Fig. 2C). In brittle frictional material, plastic shear bands form at an angle of approximately  $35^\circ$  to the direction of shortening (Kaus, 2010), close to the theoretical  $30^\circ$  angle (for a friction coefficient of 0.6). A top view of the 3D results (Fig 2D) shows consistently that the faults are at an angle of  $35^\circ$  with respect to y-direction (shortening), and evolves in the model interior to become closer to  $45^\circ$  (internal deformation of the models and hence faults rotation). The faults observed in Model  $M_{ec}$  are vertical and do not result in crustal thinning or shortening and are thus typically strike-slip faults, with dextral and sinistral kinematics on the two conjugate sets (Fig. 2C). Furthermore, the development of strike-slip faults is theoretically predicted when the maximum and minimum stresses are horizontal. This suggests that the shortening and extension should be of roughly the same magnitude to trigger strike-slip faulting.



### 3. 3D model applied to the Aegean extension with Anatolia extrusion



120

**Figure 3:** The “Aegean-like” 3D Model  $M_{ec_t}$ : pure extension ( $V_e=1$  cm/yr) during 7.5 Ma and then shortening ( $V_c=1$  cm/yr) and extension ( $V_e=1$  cm/yr) during 7.5 Ma. 3D results present strain rate after A/ 7 Ma (only extension); B/ 8 Ma (7.5 Ma of extension and 0.5 Ma of compression), C/ 10 Ma (7.5 Ma of extension and 2.5 Ma of compression) and D/ 15 Ma (7.5 Ma of extension and 7.5 Ma of compression). Key faults: normal faults in black and strike-slips in white. The Moho is drawn as a white dashed line. The input file can be found in Faucher et al. (2024).

125



The existence of strike-slip faulting inside the entire Aegean domain (Fig. 1C) suggests an almost equal contribution of extension and shortening, but only since 15 Ma (e.g. Model M<sub>ec</sub>). An important difference between Model M<sub>ec</sub> and the Aegean is the co-existence in nature of normal faults and strike-slip faults (Fig. 1C). The tectonic history of the Aegean shows that extension occurred first (Fig 1A) followed by extension and shortening (Fig 1B). We therefore propose a new 3D model that will better fit with this Aegean tectonic history (Model M<sub>ec\_t</sub>, see Figure 3), with a two-phase evolution: a first 7.5-Myr phase with only extension (similar to Model M<sub>e</sub>, representing only extension driven slab roll back; e.g. 30-15 Ma in the Aegean, Fig. 1A), followed by a 7.5-Myr coupled extension and shortening phase (similar to model M<sub>ec</sub>, representing the coeval impact of slab roll back and Anatolia extrusion; e.g. 15-5 Ma in the Aegean, Fig. 1B).

135

At 7 Myr, model M<sub>ec\_t</sub> shows pure extension with the formation of many normal faults forming a wide-rift system. At 8 Myr, the onset of compression implies a drastic modification of the strain rate pattern, which looks more homogeneous and with ongoing activity of the three former rift systems and the development of new strike-slip faults close to the side walls where shortening is imposed. After 10 Myr (i.e. 7.5 Myr of extension followed by 2.5 Myr of equal shortening and extension), the central rift is the more active one while the two others are partly re-activated in strike-slips. After 15 Myr (i.e. 7.5 Myr of extension followed by 7.5 Myr of equal shortening and extension), the central rift remains active and the two side rifts have evolved in pure strike-slip faults. The central rift is now more limited and is entirely rimmed by strike-slip faults, with dextral slip (top-left and bottom-right corners) and sinistral slip (top-right and bottom-left corners).

#### 145 **4. Discussion and conclusion**

The 3D models presented here show how the interplay (in space and time) between the Hellenic slab rollback and the westward escape of Anatolia can explain the tectonic pattern of the Aegean. At the scale of 100 km x 100 km (e.g. model box size and approximately that of the Corinth and Evvia systems or the Cyclades, Fig. 1C), we can compare the model outcomes with some first order geological features (the model x- and y-direction corresponding to N and E in the Aegean, respectively). Model M<sub>ec\_t</sub> shows E-trending areas of strong extension, rimmed by NW-trending strike-slip faults (Fig. 3D). This feature

150





shows first-order similarities to the Aegean system: the Evvia and Corinth rifts are marked by EW active normal faults and NW-trending border fault systems with sinistral motion (Fig 1C, Papanikolaou and Royden, 2007). In both model (Fig. 3D) and nature (Fig. 1C), dextral strike-slip faults also rimmed the extended area to the North (North Anatolia Trough) and South-West (Pelagonian Fault, South Evvia fault).

155

We furthermore propose that our model results support that the dextral strike-slip faults in the Aegean system does not reflect a single fault propagation process related to extrusion during Plio-Quaternary (Armijo et al. 1999, Sternai, et al., 2014), but instead reflects a distributed deformation across the entire Aegean plate. In the Eocene-Oligocene, slab roll-back and trench retreat triggered upper plate extension only. In the Mid Miocene, the onset of the westward extrusion of Anatolia (Şengör et al. 2005) modified the Aegean extension by the creation of many strike-slip faults (NAF, Pelagonian, South Evvia, Myrthes Ikaria, Fig. 1B and C). For that period, our models show that the entire Aegean plate can internally deform by the coeval activity of normal faults (accommodating slab roll-back) and strike slip faults (accommodating Anatolia extrusion). Towards the Plio-Quaternary, the NAF becomes progressively the only active strike-slip fault and the Corinth and Evvia rifts the only active extending domains, leading to an evolving tectonic pattern that is more complex than our simple model.

165

More generally, our models suggest a possible origin of large-scale strike slip faults. Continental strike slip faults are indeed enigmatic features, with various proposed origins. The Caribbean and Alboran systems show examples of continental strike slip related to STEP faulting above slab edges or tears (Govers and Wortel, 2008, Wortel and Spakman, 2004), while the San Andrea Fault represents a continental transform at plate boundaries (Irwin et al., 1990). Our models suggest that in thin, hot upper plates, and far from slab edge or plate boundaries, strike slip faults can develop by accommodating shortening that occurs coevally with and at high angle to extension. This internal deformation of a hot upper plate with strike slip faults and normal faults seems to be a common feature in gravitational-driven extension during orogenic growth (e.g. Tibet with NS normal faults and NE-SW to E-W trending strike slip that accommodate India/Eurasia shortening, Tapponier et al., 2001) or

170



175 during collapse of orogenic system (e.g. extensional domes in Variscan belt commonly associated with strike slip faults, like  
the South Armorican Shear Zone, Gapais et al.; 2015).

### Acknowledgement

We thank the Computational Infrastructure for Geodynamics ([geodynamics.org](http://geodynamics.org)) which is funded by the National Science  
Foundation under award EAR-0949446 and EAR-1550901 for supporting the development of ASPECT. We use the  
180 Meso@LR cluster in the Université de Montpellier and the Hamilton HPC cluster at Durham University for the model  
calculations. All input files for the presented numerical models can be accessed in Faucher et al., (2024).

### Author contribution

AF, FG and JvH designed the model set-up. AF runned the models. AF, FG and JvH prepared and wrote the manuscript.

### Competing interests

185 The authors declare that they have no conflict of interest.

### References

- Armijo, R., Meyer, B., Hubert, A., and Barka, A.: Westward propagation of the North Anatolian fault into the northern  
Aegean: Timing and kinematics, *Geology*, 27, 267–270, 1999.
- Bangerth, W., Dannberg, J., Fraters, M., Gassmoeller, R., Glerum, A., Heister, T., Myhill, R., and Naliboff, J.: ASPECT:  
190 Advanced Solver for Problems in Earth's ConvecTion, User Manual,  
<https://doi.org/https://doi.org/10.6084/M9.FIGSHARE.4865333>, 2023a.
- Bangerth, W., Dannberg J., Fraters M., Gassmoeller R., Glerum A., Heister T., Myhill R., and Naliboff J.:  
Geodynamics/Aspect: ASPECT 2.5.0 (version v2.5.0). Zenodo, <https://doi.org/https://doi.org/10.5281/ZENODO.8200213>,  
2023b.
- 195 Bocchini, G. M., Brüstle, A., Becker, D., Meier, T., van Keken, P. E., Ruscic, M., Papadopoulos, G. A., Rische, M., and  
Friederich, W.: Tearing, segmentation, and backstepping of subduction in the Aegean: New insights from seismicity,  
*Tectonophysics*, 734–735, 96–118, <https://doi.org/10.1016/j.tecto.2018.04.002>, 2018.



- Brun, J.-P., Faccenna, C., Gueydan, F., Sokoutis, D., Philippon, M., Kydonakis, K., and Gorini, C.: The two-stage Aegean extension, from localized to distributed, a result of slab rollback acceleration, *Can J Earth Sci*, 53, <https://doi.org/10.1139/cjes-2015-0203>, 2016.
- Buck, W. R.: Modes of Continental Lithospheric Extension, *J Geophys Res*, 96, 20161, <https://doi.org/10.1029/91JB01485>, 1991.
- Cagnard, F., Brun, J. P., and Gapais, D.: Modes of thickening of analogue weak lithospheres, *Tectonophysics*, 421, 145–160, <https://doi.org/10.1016/j.tecto.2006.04.016>, 2006.
- 205 Cloetingh, S., van Wees, J. D., Ziegler, P. A., Lenkey, L., Beekman, F., Tesauro, M., Förster, A., Norden, B., Kaban, M., Hardebol, N., Bonté, D., Genter, A., Guillou-Frotier, L., Ter Voorde, M., Sokoutis, D., Willingshofer, E., Cornu, T., and Worum, G.: Lithosphere tectonics and thermo-mechanical properties: An integrated modelling approach for Enhanced Geothermal Systems exploration in Europe, *Earth Sci Rev*, 102, 159–206, <https://doi.org/10.1016/j.earscirev.2010.05.003>, 2010.
- 210 Faucher, A., Gueydan, F., Jolivet, M., Alsaif, M., and Célrier, B.: Dextral Strike-Slip and Normal Faulting During Middle Miocene Back-Arc Extension and Westward Anatolia Extrusion in Central Greece, *Tectonics*, 40, 1–27, <https://doi.org/10.1029/2020TC006615>, 2021.
- Gapais, D., Brun, J.-P., Gumiaux, C., Cagnard, F., Ruffet, G., and Le Carlier De Veslud, C.: Extensional tectonics in the Hercynian Armorican belt (France). An overview, *Bulletin de la Société Géologique de France*, 186, 117–129, 2015.
- 215 Govers, R. and Wortel, M. J. R.: Lithosphere tearing at STEP faults: Response to edges of subduction zones, *Earth Planet Sci Lett*, 236, 505–523, <https://doi.org/10.1016/j.epsl.2005.03.022>, 2005.
- Gueydan, F., Morency, C., and Brun, J. P.: Continental rifting as a function of lithosphere mantle strength, *Tectonophysics*, 460, 83–93, <https://doi.org/10.1016/j.tecto.2008.08.012>, 2008.
- Gutscher, M. A., Dominguez, S., De Lepinay, B. M., Pinheiro, L., Gallais, F., Babonneau, N., Cattaneo, A., Le Faou, Y., 220 Barreca, G., Micalef, A., and Rovere, M.: Tectonic expression of an active slab tear from high-resolution seismic and bathymetric data offshore Sicily (Ionian Sea), *Tectonics*, 35, 39–54, <https://doi.org/10.1002/2015TC003898>, 2016.
- Heister, T., Dannberg, J., Gassmöller, R., and Bangerth, W.: High accuracy mantle convection simulation through modern numerical methods - II: Realistic models and problems, *Geophys J Int*, 210, 833–851, <https://doi.org/10.1093/gji/ggx195>, 2017.
- 225 Kaus, B. J. P.: Factors that control the angle of shear bands in geodynamic numerical models of brittle deformation, *Tectonophysics*, 484, 36–47, <https://doi.org/10.1016/j.tecto.2009.08.042>, 2010.
- Kokkalas, S. and Aydin, A.: Is there a link between faulting and magmatism in the south-central Aegean Sea ?, *Geol Mag*, 150, 193–224, <https://doi.org/10.1017/S0016756812000453>, 2013.
- Kronbichler, M., Heister, T., and Bangerth, W.: High accuracy mantle convection simulation through modern numerical 230 methods, *Geophys J Int*, 191, 12–29, <https://doi.org/10.1111/j.1365-246X.2012.05609.x>, 2012.



- Menant, A., Sternai, P., Jolivet, L., and Guillou-frottier, L.: 3D numerical modeling of mantle flow , crustal dynamics and magma genesis associated with slab roll-back and tearing : The eastern Mediterranean case, *Earth Planet Sci Lett*, 442, 93–107, <https://doi.org/10.1016/j.epsl.2016.03.002>, 2016.
- Nuriel, P., Craddock, J., Kylander-Clark, A. R. C., Uysal, I. T., Karabacak, V., Dirik, R. K., Hacker, B. R., and Weinberger, R.: Reactivation history of the North Anatolian fault zone based on calcite age-strain analyses, *Geology*, 47, 465–469, <https://doi.org/10.1130/G45727.1>, 2019.
- Pérouse, E., Chamot-Rooke, N., Rabaute, A., Briole, P., Jouanne, F., Georgiev, I., and Dimitrov, D.: Bridging onshore and offshore present-day kinematics of central and eastern Mediterranean: Implications for crustal dynamics and mantle flow, *Geochemistry, Geophysics, Geosystems*, 13, <https://doi.org/10.1029/2012GC004289>, 2012.
- Philippon, M., Brun, J.-P., Gueydan, F., and Sokoutis, D.: The interaction between Aegean back-arc extension and Anatolia escape since Middle Miocene, *Tectonophysics*, 631, <https://doi.org/10.1016/j.tecto.2014.04.039>, 2014.
- Reilinger, R., McClusky, S., Vernant, P., Lawrence, S., Ergintav, S., Cakmak, R., Ozener, H., Kadirov, F., Guliev, I., Stepanyan, R., Nadariya, M., Hahubia, G., Mahmoud, S., Sakr, K., ArRajehi, A., Paradissis, D., Al-Aydrus, A., Prilepin, M., Guseva, T., Evren, E., Dmitrova, A., Filikov, S. V., Gomez, F., Al-Ghazzi, R., and Karam, G.: GPS constraints on continental deformation in the Africa-Arabia-Eurasia continental collision zone and implications for the dynamics of plate interactions, *J Geophys Res Solid Earth*, 111, 1–26, <https://doi.org/10.1029/2005JB004051>, 2006.
- Royden, L. and Faccenna, C.: Subduction Orogeny and the Late Cenozoic Evolution of the Mediterranean Arcs, *Annu Rev Earth Planet Sci*, 46, 261–289, <https://doi.org/10.1146/annurev-earth-060115-012419>, 2018.
- Royden, L. H. and Papanikolaou, D. J.: Slab segmentation and late Cenozoic disruption of the Hellenic arc, *Geochemistry, Geophysics, Geosystems*, 12, 1–24, <https://doi.org/10.1029/2010GC003280>, 2011.
- Rutter, E. H., Faulkner, D. R., and Burgess, R.: Structure and geological history of the Carboneras Fault Zone, SE Spain: Part of a stretching transform fault system, *J Struct Geol*, 45, 68–71, <https://doi.org/10.1016/j.jsg.2012.08.009>, 2012.
- Sakellariou, D. and Tsampouraki-Kraounaki, K.: Plio-Quaternary extension and strike-slip tectonics in the Aegean, in: *Transform Plate Boundaries and Fracture Zones*, edited by: Duarte, J., Elsevier, 2018.
- Şengör, A. M. C., Tüysüz, O., Imren, C., Sakiç, M., Eyidoğan, H., Görür, N., Le Pichon, X., and Rangin, C.: The North Anatolian Fault: A new look, *Annu Rev Earth Planet Sci*, 33, 37–112, <https://doi.org/10.1146/annurev.earth.32.101802.120415>, 2005.
- Sternai, P., Jolivet, L., Menant, A., and Gerya, T.: Driving the upper plate surface deformation by slab rollback and mantle flow, *Earth Planet Sci Lett*, 405, 110–118, <https://doi.org/10.1016/j.epsl.2014.08.023>, 2014.
- Tapponnier, P.: Oblique Stepwise Rise and Growth of the Tibet Plateau, *Science (1979)*, 294, 1671–1677, <https://doi.org/10.1126/science.105978>, 2001.
- Tirel, C., Gueydan, F., Tiberi, C., and Brun, J.-P.: Aegean crustal thickness inferred from gravity inversion. Geodynamical implications, *Earth Planet Sci Lett*, 228, <https://doi.org/10.1016/j.epsl.2004.10.023>, 2004.



William P. Irwin: 3- Geology and plate-tectonic development, in: The San Andreas Fault System, California, USGS  
265 Professional Paper 1515, 61–77, 1990.

Wortel, M. J. R.; Spakman, W.: Subduction and Slab Detachment in the Mediterranean-Carpathian Region, Science (1979),  
290, 1910–1917, <https://doi.org/10.1126/science.290.5498.1910>, 2000.